In situ investigation of formation of self-assembled nanodomain structure in lithium niobate after pulse laser irradiation

V. Ya. Shur, D. K. Kuznetsov, E. A. Mingaliev, E. M. Yakunina, A. I. Lobov et al.

Citation: Appl. Phys. Lett. **99**, 082901 (2011); doi: 10.1063/1.3628646
View online: http://dx.doi.org/10.1063/1.3628646
View Table of Contents: http://apl.aip.org/resource/1/APPLAB/v99/i8
Published by the American Institute of Physics.

In situ investigation of formation of self-assembled nanodomain structure in lithium niobate after pulse laser irradiation

V. Ya. Shur,[a] D. K. Kuznetsov, E. A. Mingaliev, E. M. Yakunina, A. I. Lobov, and A. V. Ievlev
Ferroelectric Laboratory, Institute of Physics and Applied Mathematics, Ural State University, Lenin Ave. 51, Ekaterinburg 620083, Russia

(Received 17 August 2010; accepted 4 August 2011; published online 23 August 2011)

The evolution of the self-assembled quasi-regular micro- and nanodomain structures after pulse infrared laser irradiation was studied by *in situ* optical observation. The average periods of the structures are much less than the sizes of the laser spots. The polarization reversal occurs through covering of the whole irradiated area by the nets of the spatially separated nanodomain chains and microdomain rays—"hatching effect." The main stages of the anisotropic nanodomain kinetics: nucleation, growth, and branching, have been singled out. The observed abnormal domain kinetics was attributed to the action of the pyroelectric field arising during cooling after laser heating. © *2011 American Institute of Physics*. [doi:10.1063/1.3628646]

The modern development of telecommunication technologies requires fabrication of submicron- and nano-scale periodical domain structures for application in different types of optical components,[1] such as electrically controlled Bragg reflectors, beam steering devices, and narrow band filters.[2,3] Backward second harmonic generation, when the wave with the fundamental frequency propagates to the opposite direction to its second harmonic one,[4,5] needs periodically poled crystals with submicron period gratings with nanoscale accuracy of period reproducibility. Lithium niobate $LiNbO_3$ (LN) is one of the favorite ferroelectrics for domain engineering. It looks like the best candidate for nanodomain engineering. The periodically poled LN crystals are used for laser light frequency conversion based on quasi-phase-matching effect.[6,7] The fabrication of the tailored domain structures (domain engineering) is realized usually by the application of electric field and needs photolithography for electrode patterning.[8] This method is inefficient for precise domain structuring with period below 2 μm.[9]

The formation of the stable nanodomain structures in congruent LN (CLN) crystals was demonstrated experimentally under the highly non-equilibrium switching conditions.[10] Recently, the method for surface domain inversion leading to formation of the nanodomain structures has been investigated.[11] The intense ultraviolet pulse laser irradiation of single domain LN induces shallow surface nanodomain rays with width below 100 nm and depth about 2 μm. In contrast, the infrared pulse laser irradiation initiates the formation of the bulk domain structure consisting of nanodomain rays with depth up to 200 μm which is sufficient for all the above discussed practical applications.[12,13] The real progress in application of this promising original method is hindered by lack of understanding of the domain structure formation. It requires the direct *in situ* observation of the nanodomain kinetics.

In this paper, we have presented the results of *in situ* visualization of the nanodomain structure evolution induced in CLN by pulse laser irradiation.

During experiments, Z+ polar surface of the studied sample was irradiated while the domain structure was visualized by polarizing optical microscope in reflected light from Z−surface (Fig. 1). The optical contrast can be attributed to local change of the refractive index in the vicinity of the charged walls of needle-like domains due to electro-optic effect.[14,15]

The studied samples represent the 0.5-mm-thick plates of Z-cut optically polished CLN. The pulsed CO_2 laser with wavelength 10.6 μm (Versa Laser System 3.60) was used for sample irradiation by single pulse with duration ranged from 1.0 to 4.5 ms. The focusing of the laser irradiation into 0.5 to 1.0-mm-diameter spot (by ZnSe mirror and lens) allows to achieve the energy density from 5 to 30 J/cm^2. The estimated maximal temperature of the plate surface in all experiments has been below melting point for CLN which was confirmed by constancy of the surface relief in nanoscale measured before and after irradiation by atomic force microscope.

Domain structure was visualized in crossed polarizers using optical microscope (Olympus BX51). The high-speed camera (Fastcamera13) with frequency 300 fps and spatial

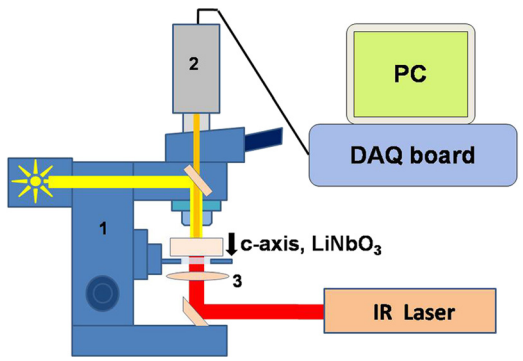

FIG. 1. (Color online) Experimental scheme for *in situ* visualization of domain structure evolution after pulse laser irradiation. 1—polarizing optical microscope; 2—high-speed camera; and 3—focusing lens.

[a]Author to whom correspondence should be addressed. Electronic mail: vladimir.shur@usu.ru.

resolution 1024×1000 pixels was used for recording the serial instantaneous domain structure images after pulse laser irradiation.

The formed static nanodomain structures were visualized with high spatial resolution using piezoelectric force microscopy (PFM) without any selective chemical etching. The avoiding of etching procedure is especially important as it was shown that the nanodomain structures can be partially destroyed by etching.[16] The PFM measurements were realized on the basis of Probe NanoLaboratory NTEGRA-Aura (NT-MDT, Russia).

The domain depth (length in the polar direction) measured by optical microscopy at the chemically etched Y cross-sections ranged typically from 50 to 100 μm. This result has been confirmed by Raman confocal microscopy which has been used for visualization of the nanodomain structures in the bulk by layer-by-layer scanning at various depths.[17]

The optically obtained instantaneous domain structure images demonstrate good contrast and time resolution (Fig. 2). The *in situ* domain observation revealed that the formation of the self-assembled structure represents the "hatching" of the irradiated area by sparsely distributed domain "rays." The ray widening (lateral growth) was negligible within experimental spatial resolution, thus the elongation of the domain rays was the only optically observed process. The ray growth along Y direction prevails (Fig. 2). The final structure was stable without any observable back-switching (flip-back) effect.

The *in situ* observation makes it possible to measure directly the time of the structure formation ranging from 10 to 90 ms which exceeds by far the laser pulse duration (1.0-4.5 ms). Moreover, it was shown that the domain kinetics starts after the laser pulse switch off with time delay from 3 to 35 ms.

Three stages of the domain structure evolution have been revealed from the set of the successive instantaneous domain patterns: (1) nucleation, (2) growth, and (3) branching. The stage "**nucleation**" represents the appearance of optically observed isolated domains (Fig. 2(a)). The stage "**growth**" is the one dimensional growth of the single narrow domains ("rays") predominantly along corresponding Y direction (Fig. 2(b)). While tracing the elongation of the individual rays from the nucleation centers, its deceleration while approaching another ray crossing its growth direction has been revealed. The stage "**branching**" represents appearance and growth of the additional short rays ("branches") from existing rays (Fig. 2(c)).

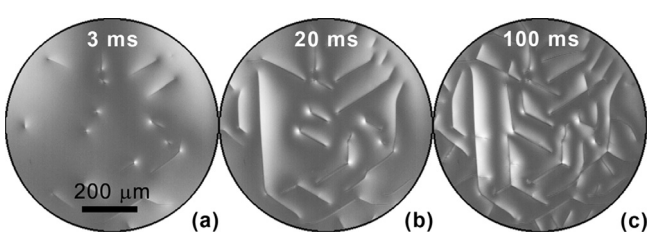

FIG. 2. Instantaneous domain structure images *in situ* observed after pulse laser irradiation. Three stages of the domain structure evolution are (a) nucleation, (b) growth, and (c) branching. Optical microscopy images in polarized light.

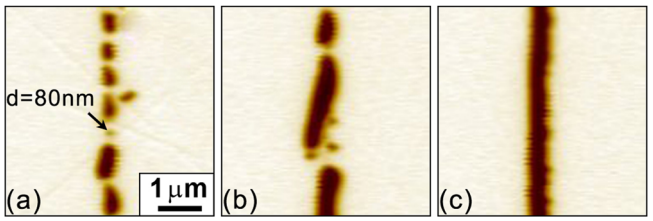

FIG. 3. (Color online) PFM images of the fragments of the static submicron domain structures: (a) chain of isolated nanodomains, (b) domain merging, and (c) domain ray.

The study of the final domain stage by high-resolution PFM method allows to reveal the fine structure of the domain rays. All growing rays represent the chains of individual nanodomains (Fig. 3(a)) transforming to continuous rays (Fig. 3(c)) as a result of subsequent merging (Fig. 3(b)). Thus, the continuous ray images obtained by optical microscopy are a result of low spatial resolution.

It was considered that the pyroelectric field E_{pyr} arising during cooling after fast heating by pulse laser irradiation plays a role of the driving force for polarization reversal, which occurs under highly non-equilibrium switching condition caused by screening retardation due to the absence of the electrodes on the surface.[18,19]

It is seen that the domain structure is spatially nonuniform along the irradiated zone. The more dense structure with randomly oriented rays appears at the edges and more sparse structure with strictly oriented along Y-direction rays—in the center (Fig. 2). This fact is due to heterogeneous distribution of the laser light density along the irradiated zone. The statistical treatment of the final domain images allows to extract the dependence of the ray growth anisotropy (fraction of Y-oriented rays) on the distance from the center of irradiated zone (Fig. 4). It was shown earlier that this anisotropy is strongly dependent on the value of E_{pyr}.[20] The obtained results (Fig. 4) demonstrate that the switching field is uniform only in the central part of the irradiated zone.

For explanation of the domain kinetics in the central part of the irradiated zone, we calculated the temperature dependence of E_{pyr} in LN crystals for uniform cyclic temperature treatment by heating and subsequent cooling. The time and temperature dependent pyroelectric field $E_{pyr}(T,t)$ was estimated as a sum of depolarization field $E_{dep}(T(t))$

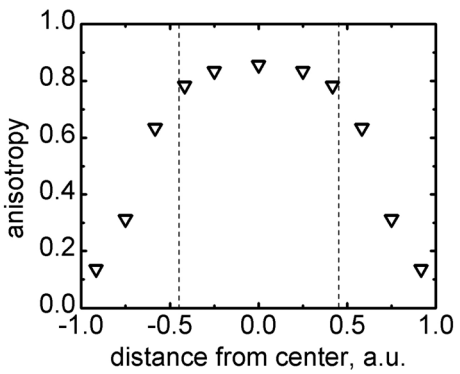

FIG. 4. The dependence of the anisotropy of ray orientation on the distance from the center of irradiated zone.

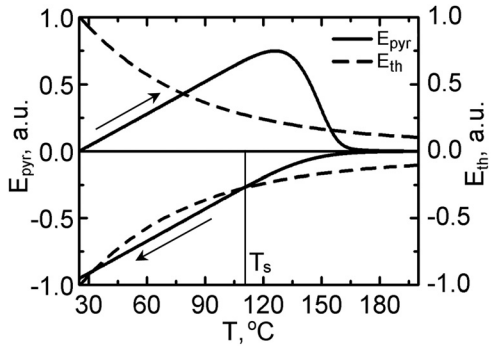

FIG. 5. Calculated temperature hysteresis of pyroelectric field for uniform heating and cooling with rate 10 °C/min (straight line) and experimental temperature dependence of nucleation threshold field (dashed line).

produced by bound charges and screening field $E_{scr}(t(T))$ produced by bulk charges

$$E_{pyr}(T,t) = E_{dep}(T(t)) - E_{scr}(t(T)). \quad (1)$$

The temperature dependence of the bulk conductivity with impurity and ionic components was taken into account

$$\sigma(T) = \sigma_{im}\exp(-W_{ac}^{im}/kT) + \sigma_{ion}\exp(-W_{ac}^{ion}/kT), \quad (2)$$

where W_{ac}^{im} and W_{ac}^{ion} are activation energies for impurity and ionic components of bulk conductivity, respectively.

The fast increase of the bulk ionic conductivity while heating above 150 °C leads to fast decrease of E_{pyr}. Thus, its value even for fast heating becomes negligible for temperatures above 200 °C. During subsequent cooling, the temperature hysteresis is observed as far as E_{dep} prevails and E_{pyr} changes the sign.

Polarization reversal started during cooling at the switching temperature T_s, when value of E_{pyr} overcame the value of temperature dependent threshold field $E_{th}(T)$ (Fig. 5).[21] The observed time delay after the end of the laser pulse and start of the domain kinetics is equal to the time required for cooling from the maximum temperature to T_s.

The nonuniform multiply surface heating by pulse laser irradiation using periodic stripe metal contact mask allowed us to produce the periodic domain structure with domain width and period exactly specified by mask and with average domain depth above 100 μm (Fig. 6).

In conclusion, the *in situ* visualization of the nanodomain structure evolution induced in congruent lithium niobate by pulse laser heating allows to investigate the formation of the bulk micro- and nanodomain structures. It was proved that polarization reversal occurred during subsequent cooling through the evolution of the self-assembled regular structures consisting of nanodomain chains. It was revealed that the anisotropic nanodomain chain kinetics consists of three main stages: nucleation, chain growth, and chain branching. The obtained results have been attributed to domain kinetics in highly non-equilibrium switching conditions under the action of pyroelectric field. The temperature hysteresis of pyroelectric field was confirmed by calculations. The spatially nonuniform pulse irradiation was used for manufacturing of the regular bulk domain structures.

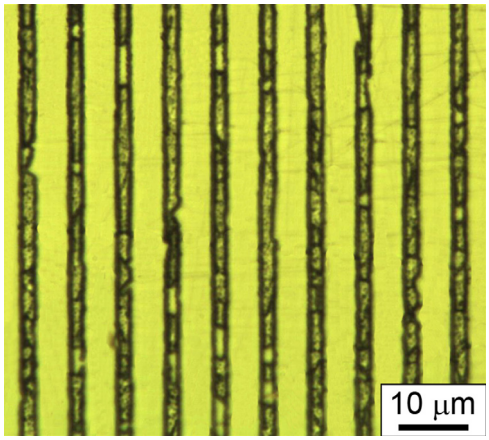

FIG. 6. (Color online) Regular domain structure formed by spatially nonuniform multiply infrared laser pulse irradiation. Optical visualization after chemical etching.

The research was supported in part by RFBR (Grs 10-02-96042-r-Ural-a, 10-02-00627-a, 11-02-91066-CNRS-a); by the Ministry of Education and Science: (16.552.11.7020, P870, P1262) and the Program UrFU (2.1.1./20).

[1]M. Yamada, M. Saitoh, and H. Ooki, Appl. Phys. Lett. **69**, 3659 (1996).
[2]J. A. Abernethy, C. B. E. Gawith, R. W. Eason, and P. G. R. Smith, Appl. Phys. Lett. **81**, 2514 (2002).
[3]C. Canalias, V. Pasiskevicius, R. Clemens, and F. Laurell, Appl. Phys. Lett. **82**, 4233 (2003).
[4]S. E. Harris, Appl. Phys. Lett. **9**, 114 (1966).
[5]S. Stivala, A. C. Busacca, L. Curcio, R. L. Oliveri, S. Riva-Sanseverino, and G. Assanto, Appl. Phys. Lett. **96**, 1111100 (2010).
[6]J. A. Armstrong, N. Bloembergen, J. Ducuing, and P. S. Pershan, Phys. Rev. **127**, 1918 (1962).
[7]D. S. Hum and M. M. Fejer, C. R. Phys. **8**, 180 (2007).
[8]M. Yamada, N. Nada, M. Saitoh, and K. Watanabe, Appl. Phys. Lett. **62**, 435 (1993).
[9]V. Shur, E. Rumyantsev, R. Batchko, G. Miller, M. Fejer, and R. Byer, Ferroelectrics **221**, 157 (1999).
[10]V. Ya. Shur, E. L. Rumyantsev, E. V. Nikolaeva, E. I. Shishkin, D. V. Fursov, R. G. Batchko, L. A. Eyres, M. M. Fejer, and R. L. Byer, Appl. Phys. Lett. **76**, 143 (2000).
[11]C. E. Valdivia, C. L. Sones, J. G. Scott, S. Mailis, R. W. Eason, D. A. Scrymgeour, V. Gopalan, T. Jungk, E. Soergel, and I. Clark, Appl. Phys. Lett. **86**, 022906 (2005).
[12]V. Ya. Shur, D. K. Kuznetsov, A. I. Lobov, E. V. Nikolaeva, M. A. Dolbilov, A. N. Orlov, and V. V. Osipov, Ferroelectrics **341**, 85 (2006).
[13]D. K. Kuznetsov, V. Ya. Shur, S. A. Negashev, A. I. Lobov, D. V. Pelegov, E. I. Shishkin, P. S. Zelenovskiy, M. G. Ivanov, and V. V. Osipov, Ferroelectrics **373**, 133 (2008).
[14]A. M. Prokhorov and Y. S. Kuzminov, *Physics and Chemistry of Crystalline Lithium Niobate* (Adam Hilger, Bristol, 1990).
[15]V. Gopalan, Q. X. Jia, and T. E. Mitchell, Appl. Phys. Lett. **75**, 2482 (1999).
[16]V. Ya. Shur, A. I. Lobov, A. G. Shur, S. Kurimura, Y. Nomura, K. Terabe, X. Y. Liu, and K. Kitamura, Appl. Phys. Lett. **87**, 022905 (2005).
[17]P. Zelenovskiy, M. Fontana, V. Shur, P. Bourson, and D. Kuznetsov, Appl. Phys. A **99**, 741 (2010).
[18]V. Ya. Shur, J. Mater. Sci. **41**, 199 (2006).
[19]A. I. Lobov, V. Ya. Shur, D. K. Kuznetsov, S. A. Negashev, D. V. Pelegov, E. I. Shishkin, and P. S. Zelenovskiy, Ferroelectrics **373**, 99 (2008).
[20]D. K. Kuznetsov, V. Ya. Shur, E. A. Mingaliev, S. A. Negashev, A. I. Lobov, E. L. Rumyantsev, and P. A. Novikov, Ferroelectrics **398**, 49 (2010).
[21]H. Ishizuki, I. Shoji, and T. Taira, Appl. Phys. Lett. **82**, 4062 (2003).